

REPRODUCIBILITY OF 7T MRI MEASUREMENTS OF THE VOLUME OF LEFT AND RIGHT HEMISPHERE OF THE HIPPOCAMPAL SUBFIELDS

Oluwatobi Folorunsho Adeyemi

University Of Abuja Nigeria

DOI: <https://doi.org/10.56293/IJASR.2024.5807>

IJASR 2024

VOLUME 7

ISSUE 2 MARCH – APRIL

ISSN: 2581-7876

**Abstract:** The hippocampus, vital for memory and spatial cognition, faces susceptibility to metabolic stress and early degeneration in neurological disorders like Alzheimer's disease (AD). This paper explores the reproducibility of high-resolution 7T MRI measurements in hippocampal subfields using the UK7T travelling head study dataset. Leveraging the Automatic Segmentation of Hippocampal Subfields (ASHS) software, subfields (CA1-3, TAIL, DG, SUB, ERC) were segmented, with exclusion of the CYST compartment. Ten healthy volunteers underwent scanning across five sites employing various scanners. Imaging protocols encompassed QSM, T1-weighted 3D-MP2RAGE, and T2-weighted sequences. ASHS segmentation required approximately 3 hours per participant. The study scrutinized 50 datasets, yielding TIV-scaled volume values. Intraclass Correlation Coefficients (ICC) were computed to gauge reproducibility. Notably, CA1 exhibited the highest ICC (0.997) for the right hippocampus, followed closely by TAIL (0.986), indicating excellent agreement. Comparable trends were observed in the left hippocampus. Overall, most subfields demonstrated very good to excellent agreement (ICC range: 0.867-0.997), implying robust measurement reliability. These findings underscore the importance of studying hippocampal subfield reproducibility in longitudinal studies, offering insights into neuroimaging advancements and potential implications for precision medicine in neurological conditions.

**Keywords:** Hippocampus, Magnetic Resonance Imaging (MRI), High-resolution Imaging, Alzheimer's Disease, Hippocampal Subfields, Automatic Segmentation, 7T MRI

INTRODUCTION

The hippocampus is an important brain structure located deep in the medial temporal lobes on both sides of the brainstem near to the cerebellum. It is involved in many brain functions such as memory and spatial reasoning (Manjon et al., 2020). The hippocampus, and in particular the CA1 sub-region (CA = cornu ammonis), is vulnerable to metabolic stress, a process which can be observed in acute neurological disorders such as ischaemia, limbic encephalitis, hypoglycaemic encephalopathy, epilepsy, multiple sclerosis, and transient global amnesia. (Thorsten, 2012). Alzheimer's disease (AD) is a neurodegenerative disease which shows early degeneration of the hippocampus (Braak & Braak, 1991). Furthermore, estimation of the volume of the hippocampus is considered a valuable tool for follow-up and treatment adjustment (Jack et al., 2005).

Studies utilizing volumetric analysis (Strange et al., 2014), histopathological examination (Braak & Braak, 1991), and molecular investigations (Genon et al., 2021) have indicated that the dorsal (or posterior) segment of the hippocampus is involved in memory encoding and spatial navigation, while the ventral (or anterior) portion plays a role in regulating emotional behaviors such as mood and anxiety. Various subregions of the hippocampus, including the Cornus Ammonis (CA 1-3), Dentate Gyrus (DG), Subiculum (SUB), and the Entorhinal Cortex (ERC), which serves as a link between the hippocampus and neocortex within the medial temporal lobe, have been scrutinized concerning their association with neurocognitive alterations in Alzheimer's disease (Birkl et al., 2015; Fyhn et al., 2004; Hett et al., 2019; Mueller et al., 2018).

In this study, we have characterised the reproducibility of high-resolution 7T volumetric measurements in the sub-fields of the hippocampus, specifically focusing upon the Cornu Ammonis (CA1-3), the tail of the hippocampus (TAIL), the dentate gyrus (DG), the subiculum (SUB) and the entorhinal cortex (ERC). The UK7T travelling head study data set (Clarke et al., 2020) was used for this study, which was carried out in preparation for measurements of longitudinal changes in the hippocampal sub-fields in Alzheimer's disease.

The segmentation of the hippocampus was accomplished through the utilization of the open-source Automatic Segmentation of Hippocampal Subfields (ASHS) software, as developed by Yushkevich and colleagues in 2015 (Yushkevich et al., 2015). The ASHS methodology employs a sophisticated pipeline that amalgamates multi-atlas label fusion with learning-based error correction techniques, creating a robust and accurate approach for hippocampal subfield segmentation (Wisse et al. 2014; Yushkevich et al. 2015).

**AUTOMATIC SEGMENTATION OF HIPPOCAMPAL SUBFIELDS (ASHS)**

The ASHS software delineates a comprehensive set of hippocampal subfields, which encompass the Cornu Ammonis (CA) areas including CA1, CA2, and CA3, the hippocampal tail (TAIL), Dentate Gyrus (DG), Subiculum (SUB), CYST, and Entorhinal Cortex (ERC). Each subfield's volume (measured in mm<sup>3</sup>) was quantified for every scan. The CYST compartment, corresponding to fluid-filled cysts, was notably absent in all images, which aligns with expectations for a cohort of young, normal volunteers. As a result, this region of interest (ROI) was excluded from the study's scope.

To provide visual context, Fig 1 serves as an illustrative representation of the ASHS segmentation process. Specifically, the ASHS-derived segmentation outcomes are superimposed onto TSE (Turbo Spin Echo) image data, offering a visualization of the delineation of hippocampal subfields.

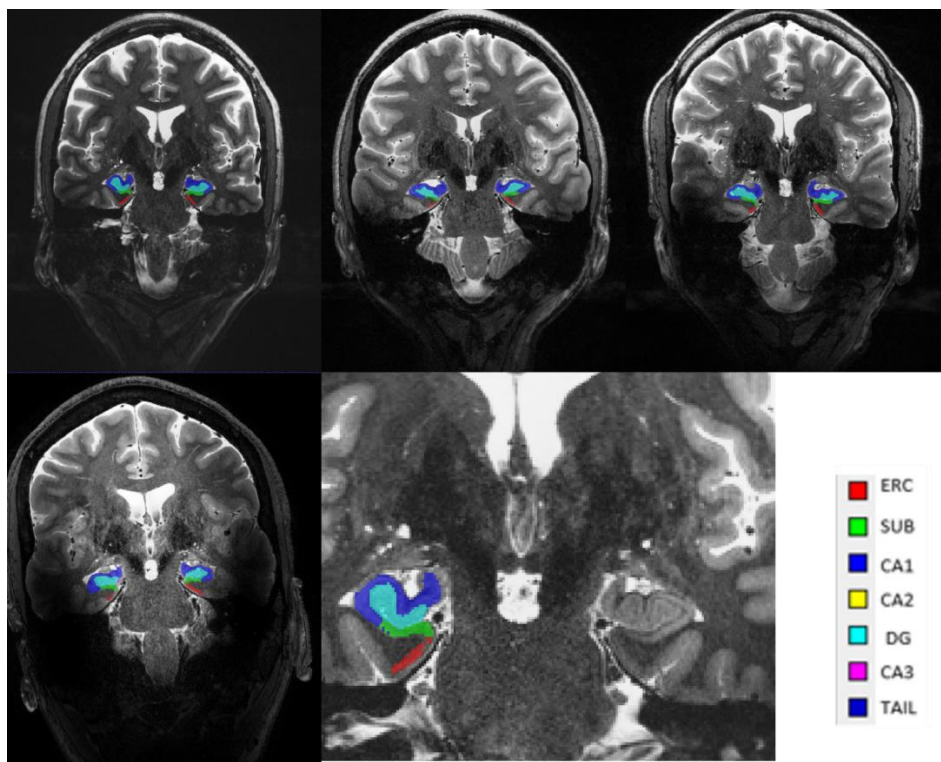


**Figure 1: TSE images showing the segmented subfields of the hippocampus of one participant from each of the 5 sites in this study (A) Subj01 (B) Subj03 (C) Subj05 (D) Subj07 and (E) Subj09.**

**IMAGING PROTOCOL**

Ten healthy volunteers (age 32 ± 6 years) were scanned with informed consent and ethics approval for a multi-site study. Two participants were scanned at each site: subj01 and subj02 were scanned at the Wolfson Brain Imaging Centre, University of Cambridge, subj03 and subj04 at the Cardiff University Brain Research Imaging Centre, Cardiff University, subj05 and subj06 at the Imaging Centre of Excellence, University of Glasgow, subj07 and subj08 at the Sir Peter Mansfield Imaging Centre, University of Nottingham and subj09 and subj10 at the Wellcome Centre for Integrative Neuroimaging (FMRIB), University of Oxford. Each subject was scanned five times at their “home” site using the scanners shown in Table 1 below.

Table 1: Scanner systems used at each site for data acquisition in the UK7T travelling head study.

	Location	Vendor	model	Software
1	Wellcome Centre for Integrative Neuroimaging (FMRIB), University of Oxford	Siemens	Magnetom 7T	VB17A
2	Cardiff University Brain Research Imaging Centre, Cardiff University	Siemens	Magnetom 7T	VB17A
3	Sir Peter Mansfield Imaging Centre, University of Nottingham	Philips	Achieva 7T	R5.1.7.0
4	Wolfson Brain Imaging Centre, University of Cambridge	Siemens	Magnetom Terra	VE11U
5	Imaging Centre of Excellence, University of Glasgow	Siemens	Magnetom Terra	VE11U

All scanners used in the data acquisition were equipped with a Nova Medical (Wilmington MA, USA) single-channel transmit, 32-channel receive (1Tx; 32Rx) head coil. All protocols were optimised for use with this coil. The image acquisition used for QSM was a whole-brain, 3D, single-echo GE sequence with an echo time of 20 ms. Additional imaging parameters were: repetition time (TR)=43 ms; Field of view  $224 \times 224 \times 224 \text{ mm}^3$ , voxel size,  $0.7 \times 0.7 \times 0.7 \text{ mm}^3$ , and frequency per pixel of 70 Hz. The data acquisition time for this sequence was 12:38 minutes (Clarke et al., 2020).

A  $T_1$ -weighted 3D-MP2RAGE image data set was also acquired for each subject. The following acquisition parameters were used: inversion times of 725/2150 ms; echo time (TE) of 2.64 ms; TR= 3500 ms; Field of view  $224 \times 224 \times 224 \text{ mm}^3$ ;  $0.8 \times 0.8 \times 0.8 \text{ mm}^3$  voxel size; receiver bandwidth of 300 Hz; the total time for this scan was 7:51 minutes, as described in (Clarke et al., 2020).

$T_2$ -weighted images spanning the hippocampus were also acquired from each subject. The acquisition parameters were as follows: partial brain TSE sequence, with a resolution of  $0.4 \times 0.4 \times 1.0 \text{ mm}^3$ ; field of view of  $224 \times 224 \times 55 \text{ mm}^3$ ; TR = 8020ms; TE = 76 ms and a bandwidth per pixel of 155 Hz. The acquisition time for this sequence was 4:32 minutes. (Clarke et al., 2020). The slice orientation was chosen so that the slices ran orthogonal to the longest axis of the hippocampus.

RESULTS

In this analysis, a total of 50 datasets were considered, corresponding to the five repeat measurements acquired on 10 subjects at the 5 different UK7T sites in the travelling head study. Segmentation of the hippocampal subfields using the ASHS software took about 3 hours for each participant's data.

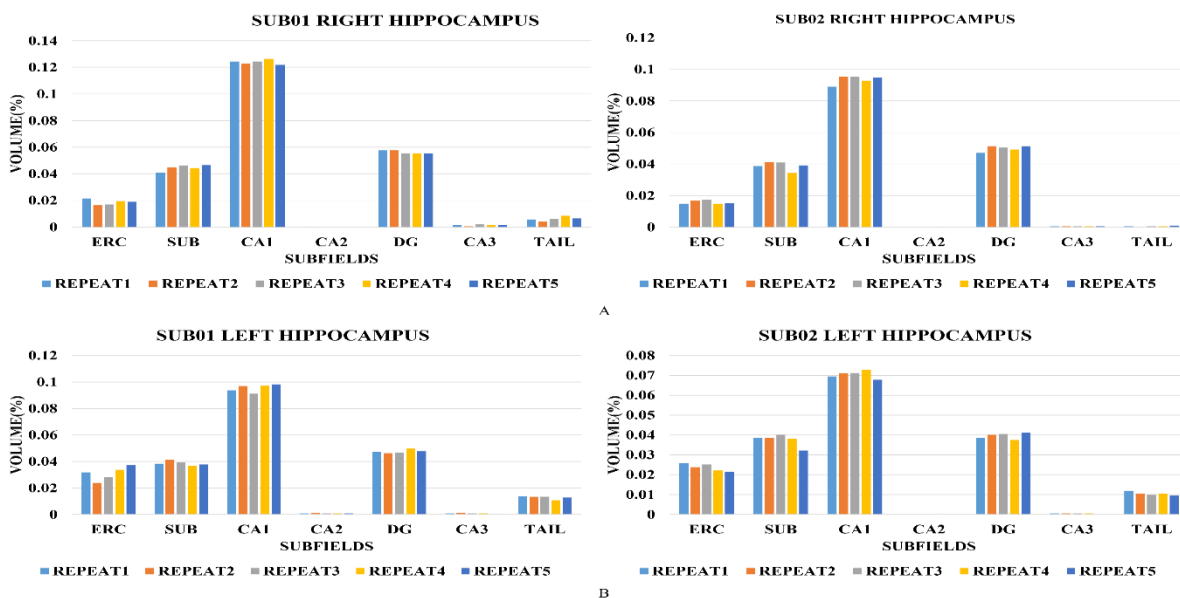


Figure 2 illustrates the TIV-scaled volume values for each subfield, obtained from the five scans conducted on two participants in this study.

Figure 2 show the repeatability graph for the left and right hippocampus value to the two participants with the intra class correlation value (ICC) shown in table 2 below.

**Table 2: showing the ICC value for the right and left hippocampus subfield measured.**

SUBFIELDS	ICC VALUE FOR RIGHT HIPPOCAMPUS	ICC VALUE FOR LEFT HIPPOCAMPUS
ERC	0.762	0.856
SUB	0.942	0.942
CA1	0.997	0.996
CA2	0.867	0.994
DG	0.965	0.978
CA3	0.959	0.904
TAIL	0.986	0.919

## DISCUSSION

This study has characterised the reproducibility of hippocampal subfield, which is important information to know before embarking on longitudinal studies involving individuals with Alzheimer's disease. By utilizing high-resolution scans at 7T scanners and implementing ASHS for precise subfield segmentation, the research quantified hippocampal subfield with a reasonable degree of consistency.

The study described here identified certain limitations in ASHS segmentation, particularly in smaller structures CYST. To mitigate this, the study combined some of these structures to volume values. For the CYST compartment, largely absent in young, normal volunteers, was excluded.

The ICC (Intraclass Correlation Coefficient) values presented in the table indicate the degree of agreement or consistency in volume measurements of hippocampal subfields between repeated scans. A higher ICC value closer to 1 suggests greater reliability and consistency in measurements.

- For the right hippocampus:
  - Among the subfields, CA1 exhibits the highest ICC value of 0.997, indicating excellent agreement between repeated measurements.
  - This is followed by the TAIL subfield with an ICC value of 0.986, also indicating excellent agreement.
  - Other subfields such as DG (ICC = 0.965), SUB (ICC = 0.942), and CA3 (ICC = 0.959) also show very good to excellent agreement.
- For the left hippocampus:
  - Similar to the right hippocampus, CA1 exhibits the highest ICC value of 0.996, indicating excellent agreement between repeated measurements.
  - The TAIL subfield follows closely with an ICC value of 0.919, indicating good agreement.
  - Other subfields such as DG (ICC = 0.978), SUB (ICC = 0.942), and CA2 (ICC = 0.994) also demonstrate very good to excellent agreement.

Overall, these ICC values suggest high reliability and consistency in volume measurements for most hippocampal subfields between repeated scans, indicating that the method used for measurement is robust and dependable. However, slight variations in agreement across different subfields and hemispheres highlight potential differences in measurement precision or biological variability.

## CONCLUSION

In summary, this study's findings underscore the critical role of studying hippocampal subfield susceptibility and volume reproducibility when planning longitudinal studies. The ability to explore microstructural changes, comprehend brain function, detect neurological disorders early, and devise personalized treatment approaches underscores the significance of this research. By contributing to neuroimaging advancement and offering potential subfield-specific therapeutics, this study introduces new prospects for precision medicine and enhanced diagnosis and management of neurological conditions. Ultimately, the insights garnered from this research could have profound implications for our understanding of brain health and function.

## REFERENCES

1. Birkel, C., Langkammer, C., Krenn, H., Goessler, W., Ernst, C., Haybaeck, J., Stollberger, R., Fazekas, F., & Ropele, S. (2015). Iron mapping using the temperature dependency of the magnetic susceptibility. *Magnetic Resonance in Medicine*, 73(3), 1282–1288. <https://doi.org/10.1002/mrm.25236>
2. Braak, H., & Braak, E. (1991). Acta H ' pathologica Neuropathological staging of Alzheimer-related changes. In *Acta Neuropathol* (Vol. 82).
3. Clarke, W. T., Mouglin, O., Driver, I. D., Rua, C., Morgan, A. T., Asghar, M., Clare, S., Francis, S., Wise, R. G., Rodgers, C. T., Carpenter, A., Muir, K., & Bowtell, R. (2020). Multi-site harmonization of 7 tesla MRI neuroimaging protocols. *NeuroImage*, 206. <https://doi.org/10.1016/j.neuroimage.2019.116335>
4. Fyhn, M., Molden, S., Witter, M. P., Moser, E. I., & Moser, M. B. (2004). Spatial representation in the entorhinal cortex. *Science*, 305(5688), 1258–1264. <https://doi.org/10.1126/science.1099901>
5. Genon, S., Bernhardt, B. C., La Joie, R., Amunts, K., & Eickhoff, S. B. (2021). The many dimensions of human hippocampal organization and (dys)function. *Trends in Neurosciences*, 44(12), 977–989. <https://doi.org/10.1016/j.tins.2021.10.003>
6. Hett, K., Ta, V. T., Catheline, G., Tourdias, T., Manjón, J. V., Coupé, P., Weiner, M. W., Aisen, P., Petersen, R., Jack, C. R., Jagust, W., Trojanowki, J. Q., Toga, A. W., Beckett, L., Green, R. C., Saykin, A. J., Morris, J., Shaw, L. M., Khachaturian, Z., ... Fargher, K. (2019). Multimodal Hippocampal Subfield Grading For Alzheimer's Disease Classification. *Scientific Reports*, 9(1), 1–16. <https://doi.org/10.1038/s41598-019-49970-9>
7. Jack, C. R., Wengenack, T. M., Reyes, D. A., Garwood, M., Curran, G. L., Borowski, B. J., Lin, J., Preboske, G. M., Holasek, S. S., Adriany, G., & Poduslo, J. F. (2005). *Neurobiology of Disease In Vivo Magnetic Resonance Microimaging of Individual Amyloid Plaques in Alzheimer's Transgenic Mice*. <https://doi.org/10.1523/JNEUROSCI.2588-05.2005>
8. Manjon, J. V., Romero, J. E., & Coupe, P. (2020). *DeepHIPS: A novel Deep Learning based Hippocampus Subfield Segmentation method*. February. <http://arxiv.org/abs/2001.11789>
9. Mueller, S. G., Yushkevich, P. A., Das, S., Wang, L., Van Leemput, K., Iglesias, J. E., Alpert, K., Mezher, A., Ng, P., Paz, K., & Weiner, M. W. (2018). Systematic comparison of different techniques to measure hippocampal subfield volumes in ADNI2. *NeuroImage: Clinical*, 17(December 2017), 1006–1018. <https://doi.org/10.1016/j.nicl.2017.12.036>
10. Strange, B. A., Witter, M. P., Lein, E. S., & Moser, E. I. (2014). Functional organization of the hippocampal longitudinal axis. *Nature Reviews Neuroscience*, 15(10), 655–669. <https://doi.org/10.1038/nrn3785>
11. Wisse, L. E. M., Biessels, G. J., Heringa, S. M., Kuijf, H. J., Koek, D. L., Luijten, P. R., & Geerlings, M. I. (2014). Hippocampal subfield volumes at 7T in early Alzheimer's disease and normal aging. *Neurobiology of Aging*, 35(9), 2039–2045. <https://doi.org/10.1016/j.neurobiolaging.2014.02.021>
12. Yushkevich, P. A., Pluta, J. B., Wang, H., Xie, L., Ding, S. L., Gertje, E. C., Mancuso, L., Kliot, D., Das, S. R., & Wolk, D. A. (2015). Automated volumetry and regional thickness analysis of hippocampal subfields and medial temporal cortical structures in mild cognitive impairment. *Human Brain Mapping*, 36(1), 258–287. <https://doi.org/10.1002/hbm.22627>